Hydrogen Bonding and Vibrational Energy Relaxation in Water−Acetonitrile Mixtures†

Dan Cringus, Sergey Yeremenko, Maxim S. Pshenichnikov, and Douwe A. Wiersma*

Ultrafast Laser and Spectroscopy Laboratory, Materials Science Centre, University of Groningen, Nijenborgh 4, 9747 AG Groningen, The Netherlands

Received: February 3, 2004; In Final Form: May 3, 2004

We present a study of the effect of hydrogen bonding on vibrational energy relaxation of the OH-stretching mode in pure water and in water−acetonitrile mixtures. The extent of hydrogen bonding is controlled by dissolving water at various concentrations in acetonitrile. Infrared frequency-resolved pump−probe measurements were used to determine the relative abundance of hydrogen-bonded versus non-hydrogen-bonded OH bonds in water−acetonitrile mixtures. Our data show that the main pathway for vibrational relaxation of the OH-stretching mode in pure water involves the overtone of the bending mode. Hydrogen bonding is found to accelerate the population relaxation from 3 ps in dilute solutions to 700 fs in neat water, as a result of increasing overlap between donor and acceptor modes. Hydroxyl groups that initially are not hydrogen bonded have two relaxation pathways: by direct nonresonant relaxation to the bending mode with a time constant of 12 ps or by making a hydrogen bond to a neighboring water molecule first (∼2 ps) and then relaxing as a hydrogen-bonded OH oscillator.

1. Introduction

Water is a unique substance, being the medium in which most chemical reactions occur that sustain life on planet Earth. Therefore, understanding the properties of water is important. Water is also one of the major absorbers of sunlight in the Earth's atmosphere. In particular the OH-stretch vibrational mode absorbs sunlight in the range of 3000−3800 cm^{-1}. One of the important issues concerning water dynamics is the question of how the excess vibrational energy is disposed. Vibrational energy relaxation (VER) is mainly a radiationless process, ultimately leading to heating of the low-frequency thermal motions of molecules. Unveiling the relaxation mechanism implies finding the intermediate steps and routes of the energy transfer process.[1−3]

Water is a very "dynamical" fluid in the sense that the rearrangements of the local structure surrounding a water molecule occur on the subpicosecond time scale.[4−11] Vibrational relaxation dynamics in water is also very fast. For instance, the population relaxation lifetime of the OH-stretching mode of HDO molecules in liquid D_2O is about 740 fs.[12] However, this relaxation lifetime is substantially longer (tens of picoseconds) when water molecules are isolated from each other in an inert liquid solvent matrix.[13,14] Hence, vibrational population (energy) relaxation in water molecules seems to be affected by hydrogen bonding.

In general, VER in polyatomic liquids can involve several different pathways.[1−3,15−21] The most frequently encountered relaxation channel is of an intramolecular nature and is promoted by anharmonic coupling between the excited mode and other, lower frequency modes. Also, intermolecular vibration−vibration and vibration−translation (rotation) energy transfer can be important. VER in the condensed phase usually occurs on a picosecond or femtosecond time scale. Therefore, spectroscopic techniques employing ultrashort laser pulses must be used to explore such fast transient processes. In particular, pump−probe spectroscopy is a useful tool to examine VER dynamics.[12,19,22]

Several previous experimental and theoretical studies focused on vibrational dynamics in water and similar hydrogen-bonded systems.[2,3,12,23−26] Pump−probe experiments on liquid water with 100 ps infrared (IR) pulses allowed only a rough estimate of the population lifetime, as the population dynamics appeared to be much shorter than the available time resolution. With the use of saturation measurements with intense IR pulses, the population lifetime of the OH-stretch vibration in HDO dissolved in D_2O was estimated to be in the subpicosecond range.[26] The currently accepted lifetime for the OH-stretching mode is 740 ± 25 fs, obtained by using IR excitation and probe pulses of a few hundred femtoseconds.[12] The temperature dependence of the vibrational lifetime was found to be anomalous, increasing rather than decreasing with temperature. This phenomenon was explained in a model where the hydrogen bond is assumed to be the main accepting mode in the relaxation of the OH-stretch vibrational mode. As the temperature increases, the OH-stretch absorption spectrum shifts to higher frequencies, which implies that the hydrogen bonds weaken. The reduced coupling between the OH-stretch vibration and the hydrogen bond results in a decrease of the energy transfer rate to the hydrogen bond and, therefore, to an increase of the population lifetime. This process is analogous to the theoretically predicted and experimentally observed VER in alcohols, where energy transfer directly to the hydrogen bond leads to its subsequent rupture.[27−33]

The OH-stretching mode dynamics in heavy water has also been studied by an IR pump visible probe pulse technique.[2,23] In this method, a femtosecond IR pump pulse excites the vibrational transition while the response of the system is monitored via spontaneous Raman scattering induced by a visible probe pulse. With this method it has been shown that at early times the vibrational energy is redistributed primarily to the bending mode overtone of HDO and D_2O molecules, while only a small fraction of the energy is transferred directly to the

† Part of the special issue "Gerald Small Festschrift".

* Corresponding author. Phone: +31-50-3634159. Fax: +31-50-3634441. E-mail: D.A.Wiersma@chem.rug.nl.

10.1021/jp0495141 CCC: $27.50
Published on Web 06/04/2004

hydrogen bond. This conclusion corroborates the results of MD simulations in which the relaxation pathway from the excited OH-stretching mode to the bending mode overtone and further on to the lower frequency intramolecular and solvent modes was shown to be dominant.[3,25] It should be pointed out, however, that the time resolution of this technique is limited to about 1 ps by a necessary tradeoff between temporal and spectral resolution.

In the aforementioned experiments, isotopically substituted water in the form of a solution of HDO molecules in D_2O was studied. Such isotopic mixtures have several advantages over isotopically pure water (i.e., H_2O). First, in HDO there is no splitting of the OH-stretch vibration into a symmetrical and asymmetrical mode, with a possible energy exchange between them. Second, resonant interactions between different water molecules, leading to intermolecular vibrational energy transfer,[34,35] are eliminated as well. Finally, the optical density of the sample is readily adjustable to an experimentally convenient value. As a consequence, the analysis and interpretation of the experimental data is substantially simplified.

Very recently, the first IR pump−probe experiments on VER in pure H_2O have been reported.[24,36] These experiments showed that the dominant mechanism of VER in pure H_2O is energy transfer to the bending mode overtone, which occurs at a 250 fs time scale. Later it was argued[37] that the lifetime is considerably longer (∼0.7 to 1 ps), and VIR occurs to the bending mode and directly to the ground state[38] (for the ongoing discussion, see refs 39 and 40). Our measurements on the OH-stretch lifetime obtained from aqueous reverse-micellar nanodroplets yielded the value of ∼200 fs.[41] At any rate, the apparent connection between the VER rate and the presence of hydrogen bonding in water presents a way for studying the phenomenon of hydrogen bonding itself.

In this paper we present a study of the effect of hydrogen bonding on VER from the OH-stretching mode of HDO molecules in the liquid phase. To control the extent of the hydrogen-bond network, water is dissolved in an inert solvent (acetonitrile) capable of forming water solutions of any concentration. We demonstrate that IR frequency-resolved pump−probe spectroscopy allows the determination of the solution composition of the water−acetonitrile solution. The relative concentrations of the OH modes that are hydrogen bonded to water molecules and those that are non-water bonded are measured for the full concentration range of water in acetonitrile. To describe the experimental results, a model is developed that accounts for the effect of the hydrogen bonding on the process of VER in liquid water. Our data support the theory in which the relaxation channel to the bending mode overtone is dominant for VER of the OH-stretching mode of water molecules.

Binary mixtures of water and acetonitrile (CH_3CN) have been extensively studied for purely scientific interest and because of their importance to applied chemistry.[42−56] For instance, a water−acetonitrile solution is used as a solvent in liquid chromatography, hydrometallurgy, and electrochemistry. Acetonitrile is a symmetrical top with a dipole moment of ∼3.9 D.[57] Due to the presence of a partial negative charge on the nitrogen side, acetonitrile can form a hydrogen bond with water molecules through nitrogen.[44] In fact, this is the process that determines the excellent solubility of water in acetonitrile. Although hydrogen bonds between water and acetonitrile molecules are considerably weaker than those between water molecules, their formation effectively destroys the three-dimensional hydrogen-bond network of water. Therefore, in water−acetonitrile solutions the extent of hydrogen bonding

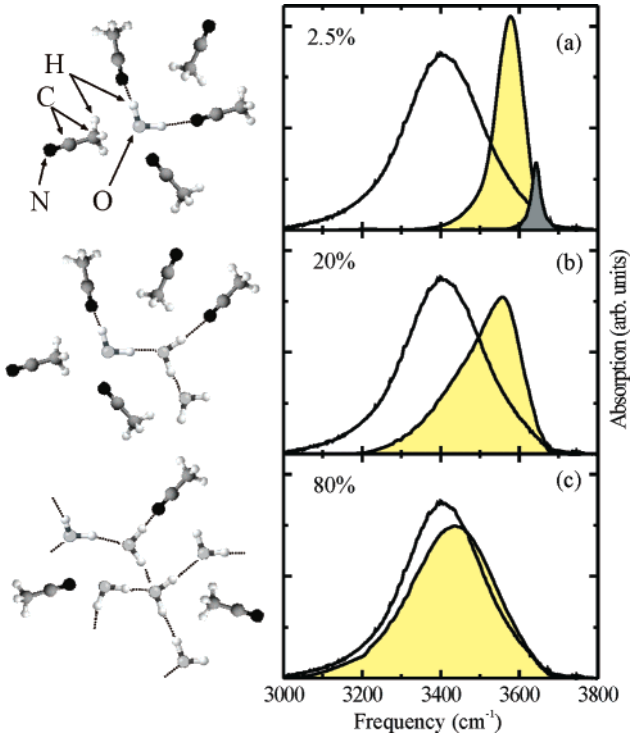

Figure 1. Spectrum of HDO molecules in the OH-stretch vibration absorption region at three concentrations of water in acetonitrile: 2.5 (a), 20 (b), and 80 (c) molar percent (shaded contours). For comparison, the spectrum of HDO in D_2O is presented by a solid curve. The spectrum of HDO molecules in CH_2Cl_2 is depicted as a dark shaded contour in (a). All spectra are corrected for the solvent contribution. At the left side of each plot the schematic representation of the characteristic unit of the sample structure is shown.

between water molecules can be controlled in a simple way. A great deal of information about the structure and properties has already been obtained using experimental methods of thermodynamics, optical spectroscopy, and electrochemistry, as well as computer simulations.[51] In light of these studies it is clear that a water−acetonitrile solution is not a simple homogeneous mixture of two components but rather a concentration-dependent structural composition. Typically, there are three main concentration regions to distinguish.[44−46,48,49,52,54] In the first region, when the molar fraction of water x_{water} is in the range of $0 < x_{water} < 0.1-0.2$, water molecules are mostly solvated by acetonitrile. The low-order water aggregates, such as dimers and trimers, begin to develop in appreciable quantities in the middle of this concentration zone. At intermediate concentrations ($0.2 < x_{water} < 0.7$) the so-called microheterogeneity sets in, meaning that relatively large water clusters are formed, and therefore, water molecules tend to be mostly surrounded by water, while acetonitrile molecules attach to acetonitrile. This tendency originates from the fact that hydrogen bonding between water molecules is stronger than between water and acetonitrile. At still higher concentrations, the structure of the solution largely resembles pure water with acetonitrile occupying vacancies in the hydrogen-bond network composed of water molecules.

The structural composition of the solution is reflected in spectroscopic data (Figure 1). At low concentrations (Figure 1a), water molecules are separated from each other and interact only with acetonitrile. MD simulations[54] indicate that on average every water molecule donates ∼1.65 hydrogen bonds while it accepts none. This results in a noticeable shift to lower frequencies and a substantial broadening of the absorption band as compared to the OH-stretch absorption spectrum in an inert solvent (Figure 1a, dark shaded contour), where there is no

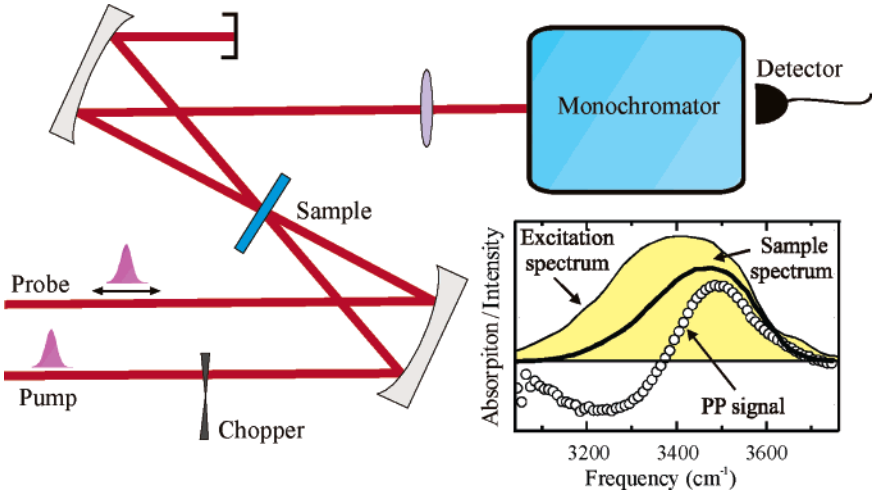

Figure 2. Schematic of the experimental setup. Examples of the sample absorption spectrum, frequency-resolved pump−probe signal, and the laser spectrum are shown in the inset.

hydrogen bond formation. However, the absorption band still remains distinctly shifted to higher frequencies with respect to its position in pure water (solid curve). Thus, the width and the position of the spectrum at this concentration are mainly determined by the interaction of water molecules with acetonitrile. The red shift compared to the gas phase absorption peak ($\sim$3700 cm^{-1})[57] indicates the formation of weak hydrogen bonds between water and acetonitrile molecules, while the narrowing of the absorption band in comparison with the spectrum of pure water is related to the different coupling strength of the OH-stretch vibrational transition and environment.

With an increase of water concentration (Figure 1b), one observes that a red-shifted wing develops in the spectrum as well as a substantial spectral broadening. This is caused by the growth of water clusters. Although the average number of donated hydrogen bonds per molecule does not change appreciably (from 1.65 in acetonitrile to 1.75 in water), the bonds become donated to other water molecules instead of acetonitrile.[54] Because the hydrogen bonds to water are stronger than to acetonitrile, the absorption spectrum develops at lower frequencies (around 3450 cm^{-1}). Also, the number of accepted hydrogen bonds increases sharply from 0 in acetonitrile to 1.75 in water as the concentration increases.[54] This results in an additional red shift and broadening of the spectrum. At concentrations exceeding 70% (Figure 1c), large clusters of water molecules have already been formed, which resemble bulk water in their properties. With a further increase of water concentration, the structure of the solution approaches the structure of pure water and the acetonitrile molecules reside primarily in voids of the water network. At this point, each water molecule accepts approximately 1.5 hydrogen bonds from other water molecules. Consequently, the position and shape of the spectrum move toward those of pure water. Nevertheless, there are still an appreciable number of acetonitrile-bonded water molecules ($\sim$15%) which results in a noticeable shoulder in the spectrum around 3570 cm^{-1}. Finally, in pure water, a water molecule both accepts and donates $\sim$1.75 hydrogen bonds. Thus, by dissolving water in acetonitrile at various concentrations, the extent and complexity of the hydrogen-bond network can be regulated.

The spectroscopic data presented in Figure 1 provide a good starting point for determining the structural composition of binary mixtures. However, as the linear spectrum is no more than a static projection of complex dynamical processes, it does not allow an unambiguous decomposition of the total absorption line into contributions from acetonitrile-bonded and water-bonded water molecules. Such decomposition is essential for grasping the relaxation pathways, since they are expected to differ for these two cases. To accomplish this, nonlinear IR spectroscopy with a femtosecond time resolution is needed.

This paper is organized as follows. In section 2, we describe the experimental setup for the IR pump−probe spectroscopy. The orientational dynamics of water molecules in an acetonitrile matrix is addressed in section 3. In section 4, experimental data on the population dynamics of water molecules are presented. In section 5, we perform a decomposition of a water−acetonitrile mixture into its components. Pathways for energy relaxation of water-bonded and non-water-bonded OH modes are outlined in section 6. Finally, in section 7, the findings are summarized.

2. Experimental Setup

The schematic representation of the experimental setup is shown in Figure 2. The IR pump and probe pulses are focused in and recollimated after the sample (100 μm free-standing jet) with two concave mirrors. The probe beam is dispersed through a monochromator (CVI) to probe the dynamics at each frequency.

The laser system is driven at a 1 kHz repetition rate. A synchronous 500 Hz chopper is inserted in the pump beam. The detected signal (modulation of the probe beam intensity ΔI^{probe}) is processed with a lock-in amplifier, while the reference signal (the probe beam intensity I^{probe}) is simultaneously detected as the dc component at the detector output. Both signals are digitized and stored in a computer. The differential absorption signal, which is called hereafter the pump−probe signal $S(t)$, is calculated as the ratio $\Delta I^{\text{probe}}/I^{\text{probe}}$.

The spectrum of the 70 fs laser pulses employed in the experiments covers both the $|0\rangle-|1\rangle$ and $|1\rangle-|2\rangle$ transitions of the chromophore—the OH-stretch vibrational mode of HDO (Figure 2, inset). This enables us to measure pump−probe signals in the required spectroscopic region without tuning the wavelength of the laser output.

The sample is prepared by mixing D_2O, H_2O, and acetonitrile volumetrically.[44] The water content in the sample is determined by the total concentration of H_2O, D_2O as well as HDO, formed due to isotopic exchange. The use of such mixtures of isotopically substituted water allows the optical density to be kept at a constant level for any concentration of water in acetonitrile. The volumes of H_2O and D_2O are chosen in such

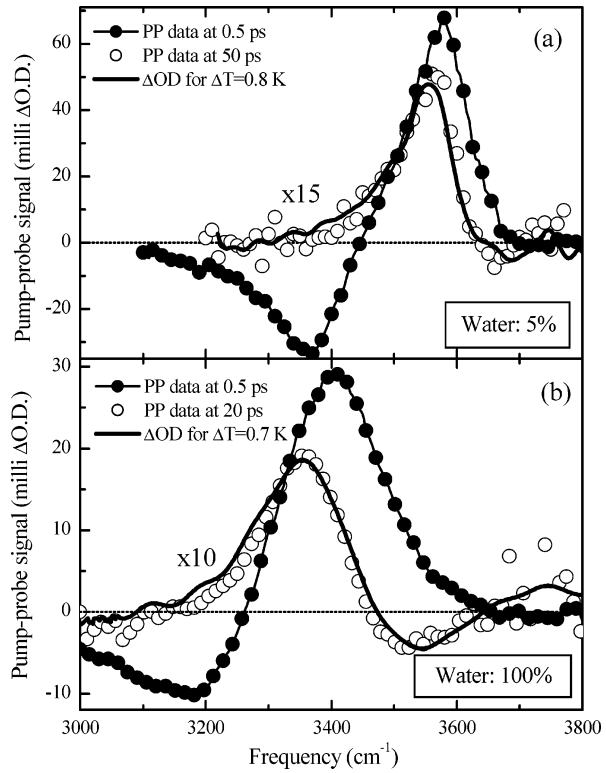

Figure 3. Transient absorption spectra for 5 molar percent of water in acetonitrile (a) and pure water (b) at short (solid circles) and long (open circles) delays. Thick solid curves show the steady-state differential absorption spectra taken at the temperature difference of 0.8 K (a) and 0.7 K (b).

a way that the concentration of HDO equals ∼0.45 mol/L in the final mixture with acetonitrile. In the most dilute solution the concentration of H_2O molecules is at least a factor of 7 smaller than the concentration of HDO. With an increasing concentration of water in acetonitrile the ratio between the concentrations of HDO and H_2O molecules gradually increases, reaching a factor of 1000 in pure water. Therefore, the content of H_2O molecules in the solution is relatively small, and the absorption in the spectroscopic region of interest (from 3000 to 4000 cm^{-1}) is mostly determined by the OH-stretch vibrational mode of HDO molecules. The chosen concentration of HDO (i.e., OH groups) leads to an optical density of ∼0.5 for a 100 μm thick sample.

For linear spectroscopy, we used a standard Fourier transform IR scanning spectrometer. The sample was contained in a 100 μm thick cell.

Two examples of experimental pump−probe signals on the OH-stretch vibrational mode of HDO in acetonitrile at 5% concentration and in D_2O are shown in Figure 3. At short delays (0.5 ps) a positive signal corresponds to an induced bleaching of the sample, which originates from the pump-induced "hole" in the ground state and stimulated emission from the excited state. A negative signal is related to the induced absorption corresponding to the transition from the excited state to the second vibrational level. The pump−probe signal decays with characteristic time scales of 10 ps (Figure 3a) and 0.7 ps (Figure 3b) until the transient spectrum reaches an asymptotic shape at 50 and 5 ps, respectively. This contour remains unchanged within experimentally accessible delays up to 0.5 ns.

The origin of the constant pump−probe signal at long delays is the following.[10,29−33] After vibrational relaxation, the energy deposited by the pump pulse is redistributed among the low-frequency modes causing a temperature rise in the focal point of the sample. This higher temperature leads to breaking of a small portion of hydrogen bonds (∼0.2% per K in neat water).[58] This results in the shift of the absorption spectrum toward higher frequencies. Because the pump−probe experiment measures the difference between sample transmission with and without the pump (i.e., the "hot" and "cold" sample), there appears an additional contribution to the pump−probe signal at short delays that originates solely from a change in the absorption spectrum. Further temperature changes are determined by the heat flow from the excitation spot and are beyond our experimental time window.

To validate this interpretation, we compared the pump−probe signals at long delays with the difference in steady-state absorption spectra measured at different temperatures (Figure 3, thick solid lines).[29,33] Both spectra can be excellently fitted when the temperature shift is 0.7−0.8 K. These values are in perfect agreement with the results of an independent estimation made on the basis of known pulse energy, the sample focal volume, and the heat capacity of the sample. The ratio in the product of heat capacity and density for water and acetonitrile of a factor of ∼2.4 is wholly compensated by the analogous ratio between the widths of the absorption spectra, which ensures that less energy is absorbed by the acetonitrile sample. We emphasize here that the amplitude of the thermal pump−probe signal provides a direct value of the temperature rise, while the signal shape is not very sensitive to temperature. This is due to the fact that the thermal shift of the spectrum is much smaller than its width, and therefore, the temperature change mostly influences the amplitude and position of the spectrum, whereas the shape of the contour is not strongly affected.

The general conclusion from the considerations above is that the ultrafast pump−probe signals at long delays contain information identical to steady-state differential spectroscopy. The fraction of hydrogen bonds that is broken due to the temperature increase of ∼0.7 K is ∼0.2%, which is negligibly small compared to the fraction of initially excited OH bonds (10−20%). Nevertheless, to account for these broken bonds, we corrected all transient spectra for the pump−probe signal at long delay (or, equivalently, the respective baseline). The precise dynamics with which the thermal contribution settles in are not essential because they occur within the time when the genuine pump−probe signal exceeds by far its thermal counterpart.

As the absorption spectrum of water in acetonitrile at low concentrations is relatively narrow, the pump−probe signals around zero delay are slightly distorted by free induction decay that is considerably longer (∼150 fs) than the excitation pulse duration (70 fs). Note that the free induction decay does not pose any problems in the case of neat water where distortions around zero delay are mainly determined by coherent coupling of the pump and probe pulses. Also, the pump−probe signal around zero delay at low concentrations of water in acetonitrile is affected by H_2O molecules (∼15%) that relax at an ∼250 fs time scale.[24] To avoid any complications that can potentially introduce these factors into the dynamics studied, we analyze the signals starting from 0.5 ps on and disregard the data before this time.

3. Orientational Dynamics of Water Molecules in Acetonitrile

Orientational motion of molecules in liquids is one of the key parameters in molecular dynamics. The characteristics of orientational dynamics, obtained from polarization-resolved pump−probe measurements, provide invaluable information for understanding the nature of molecular interactions in the system.

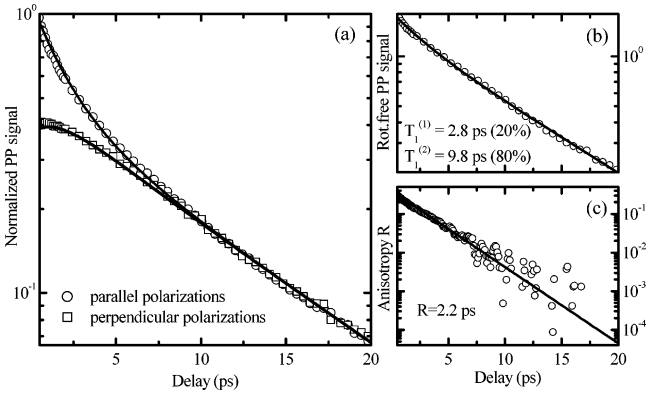

Figure 4. (a) Time-resolved pump−probe signals at the wavelength of 3550 cm^{-1} from the OH-stretch vibrational mode of HDO in acetonitrile at a concentration of 5 molar percent, measured with parallel (open circles) and perpendicular (open squares) mutual orientations of polarizations of the pump and probe pulses (left panel). The rotation-free signal (b) and orientational anisotropy (c) are calculated according to eqs 1 and 2, respectively. Solid lines in (b,c) show the best fits to the data: a biexponential function $0.2\exp(-t/T_1^{(1)}) + 0.8\exp(-t/T_1^{(2)})$ (b) and a single-exponential function with a time constant of 2.2 ps (c). The respective transients calculated with these parameters are shown in (a) as solid lines.

We therefore start the analysis of our experimental data with a discussion of the results of polarization-resolved measurements. Information about rotational dynamics of water molecules in acetonitrile is essential for the understanding of VER in this solution (vide infra).

Time-resolved pump−probe signals at a wavelength of 3550 cm^{-1} from the OH-stretch vibrational mode of HDO molecules in acetonitrile at a concentration of 5% are presented in Figure 4. As we discussed in the Introduction, at such low concentrations the aggregation of water is relatively small and therefore water molecules can be regarded as being mostly isolated from each other and only surrounded by acetonitrile. When the polarization of the pump and probe pulses is identical, the signal decays much faster than in the case of orthogonal polarizations due to rotational diffusion of the induced dipole moment. The reorientational motion completely scrambles the anisotropy by ~5 ps, and purely population relaxation dynamics dominates from then on. From the polarization-resolved data we can synthesize the rotation-free signal, that reflects population dynamics only, and the rotational anisotropy. The rotation-free signal can be calculated in the following way:[59]

$$S^{\mathrm{Rot-Free}}(t) = S(t)_{\parallel} + 2S(t)_{\perp} \qquad (1)$$

where $S(t)_{\parallel}$ and $\boldsymbol{S}(t)_{\perp}$ are pump−probe signals measured with parallel and orthogonal polarizations of the pump and probe pulses, respectively. The rotation-free signal shown in Figure 4b can be fitted by a biexponential function with time constants of 2.8 and 9.8 ps with relative contributions of 0.2 and 0.8, respectively. The slower time constant reflects the vibrational relaxation of the non-hydrogen-bonded OH oscillators while the faster constant is attributed to the hydrogen-bonded ones (vide infra).

The orientational anisotropy is found as follows:[59]

$$R(t) = \frac{S(t)_{\parallel} - S(t)_{\perp}}{S(t)_{\parallel} + 2S(t)_{\perp}} \qquad (2)$$

The orientational anisotropy of the OH-stretch vibrational mode of HDO in acetonitrile, depicted in Figure 4c, decays monoexponentially with a time constant of $\tau_R = 2.2 \pm 0.2$ ps. The pump−probe signals calculated according to the following relations

$$S(t)_{\parallel} = \frac{1}{9}[5 + 4\exp(-t/\tau_R)][(1-a)\exp(-t/T_1^{(1)}) + a\exp(-t/T_1^{(2)})]$$

$$S(t)_{\perp} = \frac{1}{9}[5 - 2\exp(-t/\tau_R)][(1-a)\exp(-t/T_1^{(1)}) + a\exp(-t/T_1^{(2)})]$$

for parallel and perpendicular polarizations, respectively, are shown in Figure 4 as solid lines.

The measurement of the orientational anisotropy of the OH-stretching mode of HDO in heavy water is considerably more challenging, since the population relaxation time is much shorter (~740 fs), limiting the dynamic range of the experimental data. We obtained a rotational diffusion constant of 3 ± 0.5 ps, in good agreement with previous experiments.[60] Interestingly enough, the rotational anisotropy does not seem to differ much for water molecules dissolved in acetonitrile and bulk water, while on basis of the substantially different hydrogen-bonding strengths one would expect a prominent effect. Most probably, the reason for this lies in the fact that the survival time of a hydrogen bond in liquid water does not exceed 1 ps.[4−10] Therefore, the hydrogen bond is broken at a time scale that is much shorter than the rotational constant, after which the molecule can rotate more or less freely. Slightly slower orientational dynamics in pure water is apparently due to stronger hydrogen bonds as well as the presence of more than one hydrogen bond per water molecule.

4. Population Dynamics of Water Molecules in an Acetonitrile Matrix

As we have already pointed out, binary mixtures of water and acetonitrile are microheterogeneous over a large concentration range. This means that the number of acetonitrile-bonded water molecules does not follow a simple linear relationship with concentration. In this section we present a decomposition analysis of water−acetonitrile mixtures obtained by frequency-resolved pump−probe spectroscopy. These data will be used in the following sections to create a self-consistent model describing the effect of hydrogen bonding on VER in pure water and acetonitrile solutions.

The experimental pump−probe signals of the OH-stretch vibrational mode of HDO in acetonitrile for several concentrations, spanning the range from 5% to pure water, are shown in Figure 5. The experiments were performed with the polarization of the pump and probe pulses set at 54.7°, which provides a signal free of orientational anisotropy and therefore reflecting only population relaxation dynamics.[61]

The left panel in Figure 5 shows transient spectra at different concentrations at a fixed delay of 500 fs where pulse overlap, free induction decay, or contributions from H_2O, do not affect the signals. With increasing concentration the transient absorption spectra shift to lower frequency and become considerably broader. This is in full agreement with the behavior of the linear absorption spectra depicted in Figure 1. Note that the separation between the peaks of induced bleaching and absorption, which is directly related to the anharmonicity parameter (i.e., the frequency difference between the $\langle 0|-\langle 1|$ and $\langle 1|-\langle 2|$ vibrational transitions), remains almost constant (~220 to 250 cm^{-1}) for any concentration. Therefore, the three-dimensional hydrogen-bond network does not substantially affect the anharmonicity

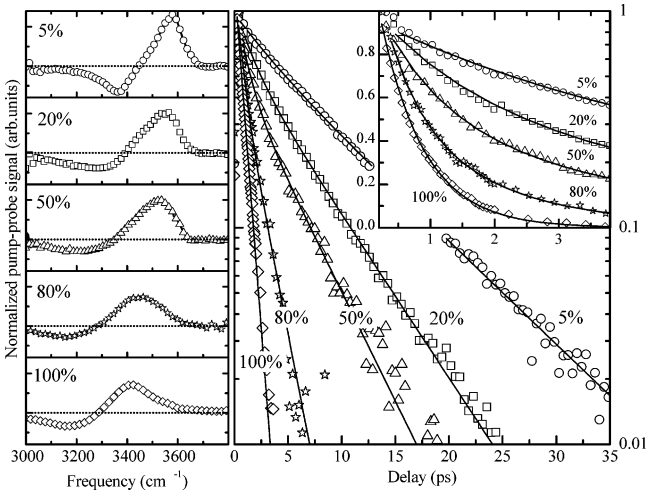

Figure 5. Pump−probe signals from the OH-stretch vibrational mode of HDO in acetonitrile at concentrations of 5, 20, 50, 80, and 100 molar percent. The left panel represents frequency-resolved pump−probe signals at a fixed delay of 500 fs. In the right panel the time-resolved pump−probe signals at 3500 cm^{-1} are shown on a logarithmic scale. All data were taken with polarization of the pump and probe pulses set at 54.7° to ensure rotation-free signals. The inset shows the first 4 ps of the transients on a linear scale.

of the OH-stretch potential energy surface, at least not in the vicinity of the two lowest transitions.

The right panel of Figure 5 represents the time-resolved transients at 3500 cm^{-1}, which is close to the peak of induced bleaching. The population lifetime substantially decreases with an increase of concentration of water in acetonitrile. It changes from ∼12 ps in dilute solutions, where the water molecules are well separated from each other, to ∼700 fs in pure water, where a complete three-dimensional hydrogen-bond network exists. Therefore, population relaxation dynamics is obviously facilitated by hydrogen bonding. Apart from that, the time-resolved pump−probe signals for intermediate concentrations do not show monoexponential dynamics but can be fitted well to a biexponential decay function (Figure 5, solid lines). This strongly suggests that there are two different types of OH bonds coexisting at the intermediate concentrations. In order to elucidate this issue we performed a series of time-resolved pump−probe scans in the whole frequency range corresponding to the absorption of the OH-stretch vibrational mode.

The result of a combined time−frequency scan for a 50% solution is presented in Figure 6. It is comprised of 11 time-resolved pump−probe transients measured in the wavelength range from 3100 to 3600 cm^{-1} with the equidistant step of 50 cm^{-1}. For the sake of clarity, all time-resolved pump−probe scans are normalized to the respective maximum value. It is clear that the signal decay rate is wavelength dependent. Within the induced bleach (induced absorption) band the signal decays slower at shorter wavelengths than at longer ones (solid curve). For this particular concentration of water in acetonitrile, the average population lifetime changes from ∼3.2 ps at the blue wing of the absorption band to ∼1.2 ps at the red one.

Such a dependence of population lifetime on wavelength is determined by the effect of diverse solvent environments for different OH bonds. The formation of a hydrogen bond between water molecules leads to the red shift of the absorption band of the OH-stretch vibration.[62] Therefore, hydroxyl groups that form a hydrogen bond to acetonitrile have higher frequencies (∼3550 cm^{-1}, Figure 1a) and, as Figure 6 shows, longer relaxation times. In contrast, hydroxyl groups that make a hydrogen bond to other water molecules have lower frequencies (∼3400 cm^{-1})[62] and

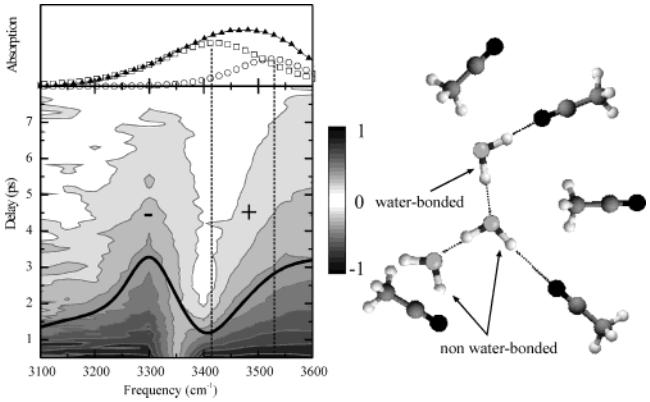

Figure 6. A representative time−frequency pump−probe scan for a 50% solution. All transients are normalized to unity at zero delay. The thick solid line in the 2D plot depicts the level at which the signal decays by a factor of 1/e. Triangles in the top plot depict the linear absorption spectrum for this concentration, while squares and circles show the spectral components corresponding to water-bonded and non-water-bonded hydroxyl groups, respectively. A schematic illustration of the microscopic structure of the solution is depicted next to the figure.

much shorter relaxation times. Hence, the biexponential decay of the time-resolved pump−probe signal at 3500 cm^{-1} for intermediate concentrations (Figure 5) can be attributed to the presence of two types of hydroxyl groups: one bonded and the other not bonded to water molecules.

5. Signal Analysis in Terms of Hydrogen-Bonded versus Non-Hydrogen-Bonded Species

We are now in a position to perform a global fit to the pump−probe data, which is based on the assumption that there is a clear separation of time scales between the dynamics of water-bonded and non-water-bonded oscillators. At any given wavelength, the pump−probe signal can be represented as a linear combination of two terms:

$$S(\omega,t) = A^{(\mathrm{bonded})}(\omega)\mathrm{e}^{-t/T_1(\mathrm{bonded})} + A^{(\mathrm{nonbonded})}(\omega)\mathrm{e}^{-t/T_1(\mathrm{nonbonded})} \quad (3)$$

The first term in eq 3 describes the pump−probe signal of hydroxyl groups that have a hydrogen bond to other water molecules. Accordingly, parameters $A^{(\mathrm{bonded})}(\omega)$ and $T_1^{(\mathrm{nonbonded})}$ express, respectively, the amplitude of the signal at the corresponding wavelength and the population lifetime. The second part of this expression describes the signal of the hydroxyl groups that are not linked by the hydrogen bond to water molecules with corresponding variables.

We have performed a global fit of the experimental data to this model, i.e., the complete time−frequency scan (similar to that depicted in Figure 6) for each concentration is simulated in a single fitting session. The parameters representing the population lifetime are global for each concentration, while the amplitudes are varied to produce pump−probe transients for each type of oscillator *independently*. This information will be used to decompose the content of the water−acetonitrile mixture into two components and verify the validity of the model.

The quality of the fit is excellent as can be judged from Figure 7, where 6 out of 11 representative transients are shown for a concentration of 50%. Note that the peculiar shape of the pump−probe signal at 3400 cm^{-1}, initially decaying from positive to negative values and later rising back to zero, is well reproduced. This behavior is related to the fact that at this wavelength the pump−probe signal consists of a positive (induced bleaching)

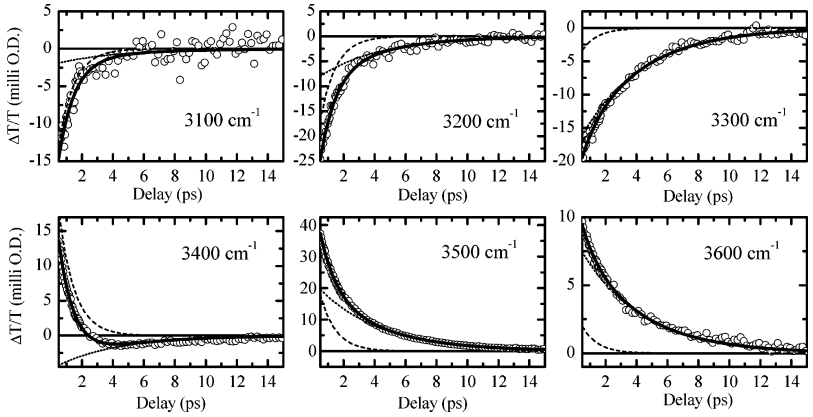

Figure 7. Fit of time-resolved pump−probe signals for a water concentration of 50%. The symbols represent the experimental data points, while the results of the simulations are shown by the solid curves. The relaxation components belonging to water-bonded and non-water-bonded OH oscillators are shown by dashed and dotted lines, respectively. Six out of the set of 11 transients are shown, while the total data set comprises nine different concentrations.

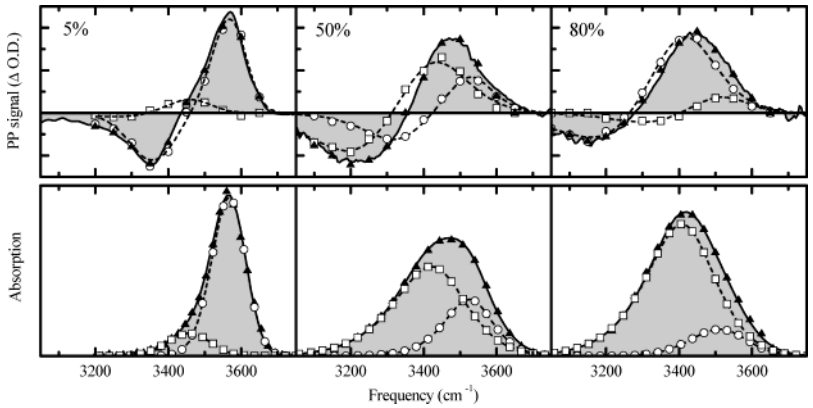

Figure 8. Decomposition of transient (top panel) and linear (bottom panel) absorption spectra onto subbands corresponding to water-bonded (open squares) and non-water-bonded (open circles) hydroxyl groups. Solid triangles represent the sum of the two components. Solid curves show independently measured transient spectra at a 500 fs delay (top panel) and linear absorption spectra (bottom panel). For details of the simulations consult the text.

component corresponding to the water-bonded hydroxyl groups (dashed line) and a negative (induced absorption) component of the non-water-bonded ones (dotted line). The non-water-bonded oscillators have a much longer (by a factor of ∼4) population lifetime, and therefore their contribution dominates at longer delays.

The fit of the experimental pump−probe data at each concentration yields the values of the population lifetimes and the spectral amplitudes of the components associated with water-bonded and non-water-bonded hydroxyl groups. We leave the detailed discussion on the population lifetimes to the next section, concentrating here on the signal analysis. This allows us to verify the validity of the applied model (eq 3) that implies that only two components suffice to describe the experimental data adequately. Two issues will be addressed: (i) whether linear absorption spectra (Figure 1) can be modeled with the same parameters and (ii) whether the results obtained from the microheterogeneity model are consistent with the MD simulations.[44,45,54]

The spectral amplitudes derived from the global fits allow the decomposition of the total frequency-resolved pump−probe signal into contributions originating from the water-bonded and non-water-bonded hydroxyl groups (Figure 8, top panel). Here, the open squares depict the amplitudes of non-water-bonded hydroxyl groups ($A^{(\text{nonbonded})}$ in eq 3) while the circles correspond to the water-bonded ones ($A^{(\text{bonded})}$ in eq 3). As expected, their sum (solid triangles) equals the respective transient spectra that have been measured independently (solid curves).

As one can see from Figure 8, at a water concentration of 5% the pump−probe signal originates mostly from the non-water-bonded hydroxyl groups. When the molar fractions of water and acetonitrile are equal, the component corresponding to the water-bonded hydroxyl groups noticeably dominates, which is a clear manifestation of the mixture's microheterogeneity. Correspondingly, at a concentration of 80% most of the pump−probe signal comes from the water-bonded hydroxyl groups.

In order to extract the components related to water-bonded and non-water-bonded hydroxyl groups from the pump−probe data we performed the following analysis. For each concentration an independently measured linear absorption spectrum and the components of the pump−probe spectrum (Figure 8, top panel) are simulated simultaneously using a global fitting procedure. The linear absorption spectrum is described as a sum of two spectral bands corresponding to the water-bonded and non-water-bonded hydroxyl groups. Each of the two pump−probe signal components is presented by a sum of two lines responsible for the induced bleaching and induced absorption. The components of the linear absorption spectrum and the signals corresponding to the induced bleaching in the pump−probe spectra (i.e., the contours related to the $|0\rangle-|1\rangle$ vibrational transition) are fitted with spectral lines of identical shapes and positions. The width and amplitude of the line corresponding to the induced absorption in the pump−probe signals are free parameters in the fit. To model the line shape we used the following asymmetric contour:

$$S(\omega) = \frac{A}{1 + a\left(\frac{\omega - \omega_0}{\delta\omega(1 + s(\omega - \omega_0))}\right)^2} \times \exp\left[-\frac{1 - a}{2}\left(\frac{\omega - \omega_0}{\delta\omega(1 + s(\omega - \omega_0))}\right)^2\right] \quad (4)$$

Here the parameters A, $\delta\omega$, ω_0, s, and a define the height, width, position, asymmetry, and balance between Gaussian (inhomogeneous) and Lorentzian (homogeneous) contributions to the line shape, respectively. The line asymmetry is related to the fact that the frequency of the OH-stretch vibrational mode is a nonlinear function of the hydrogen bond length. The asymmetry of the OH-stretch absorption line of water molecules in acetonitrile is observed even at the lowest water concentrations, when the amount of water-bonded hydroxyl groups is negligibly small (Figure 1, top panel).

The fit results are presented in the lower panel of Figure 8. The contributions to the total absorption spectrum from the non-water-bonded and water-bonded hydroxyl groups are shown by open circles and squares, respectively. With the increase of concentration of water the band that corresponds to the water-bonded hydroxyl groups gradually grows, while the contribution from non-water-bonded oscillators diminishes. At low concentrations water molecules are mostly present as monomers and dimers. The absorption spectrum of a hydroxyl group of the probe HDO molecule that is donated to a heavy water molecule peaks at ~3470 cm^{-1}. With the increase of water concentration more hydrogen bonds to other D_2O molecules are formed.[54] As a consequence, the absorption contour gradually shifts to its asymptotic value of 3400 cm^{-1}. The spectrum also broadens by ~50% as a result of distribution in the local surroundings and their dynamical fluctuations. Therefore, our analysis indicates that the OH-stretch frequency of the HDO molecule decreases by ~175 cm^{-1} as compared to the inert solvent, upon a hydrogen bond formation from the hydroxyl group under consideration. Further involvement of the HDO molecule in hydrogen bonding results in an additional ~70 cm^{-1} red shift. The latter value is also consistent with the position (~3575 cm^{-1}) of the non-hydrogen-bonded hydroxyl group in neat water.[5,62] The sum (solid triangles) of two bands corresponding to the water-bonded and non-water-bonded hydroxyl groups correctly describes the linear absorption spectra at the corresponding concentrations (solid curves). Therefore, despite the simplicity of the applied model, it is capable of reproducing the linear absorption spectra as well, which provides strong support for its validity.

The composition of the solution can be determined by assuming that the concentration of each type of OH oscillator is proportional to the integrated intensity of its spectral band. As the absorption cross section of water-bonded OH oscillators is ~30% larger than that of non-water-bonded OH oscillators, the integrated intensities were normalized in such a way that their sum equals unity. The mixture composition found in this way is presented in Figure 9 by open symbols. From the microheterogeneity model one may expect the fractions of water-bonded and non-water-bonded OH oscillators to be nonlinear functions of the molar fraction of water.[44,45,54] This is fully confirmed by the experimental results (Figure 9).

Hydrogen bonding in water−acetonitrile mixtures has been extensively studied by MD simulations (see, for instance, ref 54). Typically, three types of hydrogen-bonding states for OH groups are considered: hydrogen bonded to water, hydrogen bonded to acetonitrile, and non-hydrogen bonded. We redistributed non-hydrogen-bonded OH oscillators between water-bonded and non-water-bonded (as observed in a pump−probe experiment) in the following way. In pure water, ~15% of the OH bonds are not linked by a hydrogen bond to other water molecules.[6,63] Correspondingly, in pure acetonitrile this concentration is zero. We assume the intermediate behavior to be linear with concentration, add respective values to water-bonded and non-water-bonded fractions, and renormalize the corrected concentration functions to unity. Although a linear interpolation seems to be oversimplified, and perhaps even ill-justified from a microheterogeneity viewpoint, it cannot introduce a substantial error due to the relatively small fraction of the oscillators to be redistributed (15%). The solid curves in Figure 9 present the results of MD simulations[54] processed as described above. Our experimental data agree reasonably well with the results of the MD simulations confirming the essence of the applied model.

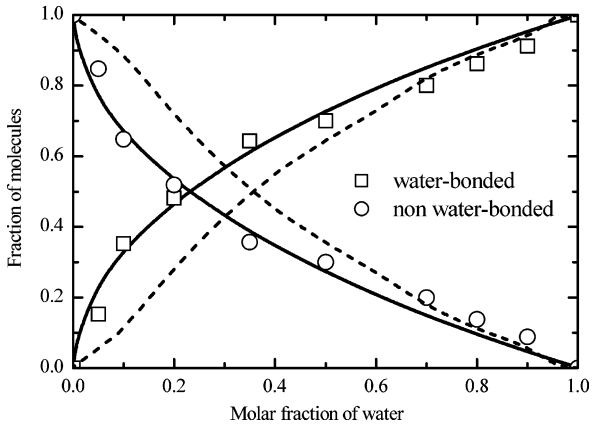

Figure 9. Dependence of solution composition on the concentration of water in acetonitrile. The symbols depict the integrated amplitudes of spectral bands corresponding to water-bonded (squares) and non-water-bonded (circles) hydroxyl groups. The solid and dashed lines show the fractions of water-bonded and non-water-bonded hydroxyl groups found in MD simulations[54] and in a linear spectroscopic experiment,[44] respectively.

It is instructive to compare the effectiveness of a mixture decomposition by means of nonlinear and linear spectroscopy.[44,45] In the latter case, the results strongly depend on the data processing procedure and the particular choice of supplementary information, as overlap of corresponding spectral components. For instance, the linear absorption spectrum at a 50% concentration is portrayed by a wide featureless band with no apparent signs of water-bonded or non-water-bonded OH oscillators (Figure 8). The dashed curves in Figure 9 show the results of the analysis of the linear spectroscopic experiment.[44] As can be seen from Figure 9, the dependence of fractions of water-bonded and non-water-bonded OH groups on the water concentration is much closer to linear in comparison with the data obtained in MD simulations and nonlinear spectroscopy. Hence, the extent of hydrogen bonding between water molecules in acetonitrile solution is substantially underestimated in the analysis of the linear spectroscopic experiment.

At this point the question may be raised why only two basic components suffice to describe steady-state and transient spectra. Although at any moment there is a wide distribution of hydrogen-bonded coupling strengths (as reflected in the broad absorption spectrum), the distribution is not static but rather dynamical. Recent photon echo experiments revealed that restructuring of bulk water occurs at the time scales of ~100 and ~700 fs with the fast component dominate (~70%).[4−10] Therefore, molecules that are strongly hydrogen bonded become weakly bonded within 100 fs, and vice versa. It is this spectral

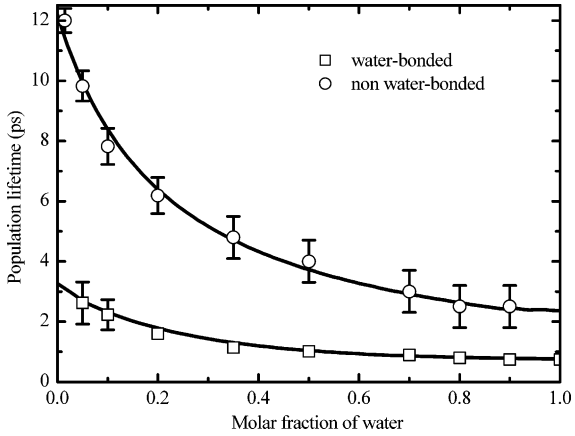

Figure 10. Concentration dependence of population lifetimes for non-water-bonded (circles) and water-bonded (squares) hydroxyl groups. The solid curves represent the results of simulations (see text for details).

scrambling, occurring at a time scale much shorter than the shortest population lifetime (~700 fs), that prevents vibrational population relaxation from being frequency dependent. At the intermediate concentration, the momentarily distribution in hydrogen-bonded coupling strengths and the number of additionally donated/accepted hydrogen bonds is contained in the central position and the width of the absorption spectrum of the already hydrogen-bonded hydroxyl groups. As far as acetonitrile-bonded HDO molecules are concerned, the absorption spectrum is much too narrow to expect any frequency-dependent relaxation. Also, the phase dynamics of the OH stretch of the HDO molecule dissolved in acetonitrile are completed far before the population relaxation takes place (see section 6). However, we would like to stress that from the spectroscopic data alone we are not able to distinguish, for instance, double-bonded water molecules from triple-bonded ones, etc. Clearly, additional MD simulations are required here to obtain a more detailed microscopic picture. Nonetheless, the partition between water- and acetonitrile-bonded water molecules does not seem to be problematic.

Summarizing this section, we conclude that ultrafast nonlinear pump−probe spectroscopy allows direct and unambiguous resolution of the sample composition with respect to water-bonded and non-water-bonded OH groups. Such a decomposition is possible because the corresponding components of the binary mixture differ by their frequency and/or time characteristics.

6. Pathways for Vibrational Energy Relaxation

Having obtained the mixture composition and the orientational dynamics of water molecules in acetonitrile, we can proceed with the investigation of the vibrational energy relaxation mechanism. The concentration dependencies of population lifetimes of non-water-bonded and water-bonded hydroxyl groups derived from the global fit according to eq 3 are shown in Figure 10. For both components the population lifetime decreases with increasing concentration: from ~12 ps to ~2.5 ps for the non-water-bonded OH oscillators and from ~3 ps to 700 fs in the case of water-bonded ones. The latter time practically sets in at a water fraction of ~0.5. Such behavior of the population lifetime is in agreement with the microheterogeneity model.[44−46,51,52] At this concentration large water aggregates, resembling bulk water, are formed. With a further increase of concentration the structure of the solution resembles more and more that of bulk water, with acetonitrile molecules residing in vacancies of the water network.

The concentration dependence of the population lifetime of water-bonded hydroxyl groups can be explained in the framework of a model that has briefly been discussed in the Introduction.[2,3,23] According to this model, the first step in the vibrational population relaxation is a near-resonant energy transfer from the excited OH-stretching mode to the first overtone of the bending mode. Further energy redistribution involves intra- and intermolecular relaxation to lower vibrational levels, hydrogen bond modes, and other low-frequency molecular motions. The relaxation rate is determined by the energy overlap between the donor and acceptor modes, which are in this case the fundamental OH-stretch vibrational transition and the first overtone of the bending mode, respectively.[1,16,19,22] According to Fermi's golden rule the relaxation rate can be expressed in the following way

$$1/T_1 \propto \int |\langle 1_v 0_\delta | V_{v\delta} | 0_v 2_\delta \rangle|^2 \, \delta(E_v - E_{2\delta}) \rho(E_v = E_{2\delta}) \, \mathrm{d}E \quad (5)$$

where $\langle 1_v|$ and $|0_v\rangle$ denote the initial and final states of the donor mode (OH-stretch), $\langle 0_\delta|$ and $|2_\delta\rangle$ the initial and final states of the acceptor mode (bending vibration), correspondingly, $V_{v\delta}$ is the interaction potential, and $\rho(E_v = E_{2\delta})$ is the density of states. Equation 5 represents the overlap integral of the spectral band corresponding to the water-bonded hydroxyl groups and the spectrum of the bending mode overtone. The former has been found from the analysis of the pump−probe data (see Figure 8). The shape and position of the latter are derived from the spectrum of the fundamental transition assuming the mode to be almost harmonic. The validity of this assumption has been discussed in detail in ref 64. The only adjustable parameter in the model turns out to be a scaling factor.

The result of the simulations is shown in Figure 10 as a solid line, which adequately reproduces the experimental data. The spectrum of the donor mode (OH-stretch) shifts to lower frequencies and broadens with an increase of the concentration of water in acetonitrile (Figure 8), which leads to a better overlap with the spectrum of the accepting mode and, consequently, a more efficient resonant energy transfer. The width and position of the bending mode spectrum are not significantly changed with variation of the concentration as compared to the corresponding parameters of the OH-stretching mode. Therefore, the alteration of the spectrum of the bending mode does not contribute much to the concentration dependence of the population lifetime. Thus, the dependence of the population relaxation time for the water-bonded OH oscillators on the concentration of water in acetonitrile is mainly determined by the modifications of the spectrum of the OH-stretching mode that, in turn, reflects the amount of hydrogen bonding and local surrounding fluctuations.

In the case of non-water-bonded hydroxyl groups, the relaxation pathways are quite different. At the lowest concentration, water molecules are separated far from each other and surrounded by acetonitrile. The absorption spectrum (Figure 1a) shifts to higher frequencies and narrows.[44,45] Its overlap with the spectrum of the bending mode overtone becomes negligible. Hence, the resonant intramolecular relaxation channel to the bending mode overtone becomes substantially less efficient, and consequently, the population lifetime reaches 12 ps in the most dilute solution. In an inert solvent, such as CH_2Cl_2, where no hydrogen bonds are formed, the absorption spectrum is shifted even further to higher frequencies and the population lifetime approaches several tens of picoseconds.[13,14] In the opposite case of a red-shifted absorption spectrum (for instance, H_2O molecules isolated in acetonitrile) the population lifetime shortens

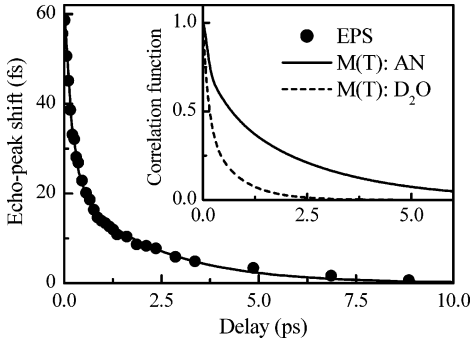

Figure 11. The echo−peak shift (EPS) function for 5% water in acetonitrile. Solid circles show the experimental points, and the line depicts the result of computer simulations with the correlation function $M(t)$ presented in the inset. The correlation function of HDO in D_2O[5,10] is also shown for comparison (dashed line).

to ∼8 ps. These facts point toward the supposition that the first step in the relaxation mechanism involves a nonresonant energy transfer to the bending mode; however, this process is not as efficient as in the case of water-bonded OH oscillators. Another possible relaxation channel is a direct relaxation to the librational modes without the bending mode as an intermediate. Also, we cannot completely rule out the possibility of energy relaxation directly to acetonitrile, mediated by a hydrogen bond.

With increasing water concentration the population relaxation lifetime of non-water-bonded molecules sharply decreases approaching an asymptotic value of ∼2.5 ps. This value is very close to the rotational anisotropy constant of HDO in acetonitrile, established in section 3, (∼2.2 ps) and water (∼3 ps).[60] This strongly suggests the following relaxation pathway: Initially a non-water-bonded OH oscillator belonging to a water molecule, which is part of a cluster, reorients and creates a hydrogen bond to another water molecule with a characteristic time of ∼2.5 ps. Consequently, the spectrum of the oscillator is modified (broadens and shifts to lower frequencies) and the resonant energy relaxation channel opens to the bending mode overtone. The energy in this case is transferred to the donor mode at a time scale of ∼700 fs. The latter process is substantially faster than the reorientation time, and therefore the relaxation rate is mainly determined by the reorientation time.

To confirm the feasibility of such a pathway, we performed IR vibrational echo−peak shift measurements[8−10,65] on HDO dissolved in acetonitrile (Figure 11). It appears that the echo−peak shift function decays at time scales of ∼250 fs and ∼2 ps, which is consistent with our heterodyne-detected echo experiments.[5] The solvent-related thermal effects that substantially distort echo peak shift measurements in neat water[8,10] do not present any problem in acetonitrile because the population relaxation time is much longer than the phase dynamics. The frequency correlation function calculated from the echo−peak shift and heterodyned two-pulse photon echo experiments is shown in the inset to Figure 11. It can be represented by a biexponential function with characteristic times of ∼240 fs (40%) and ∼2.3 ps (60%). The fast time originates from fluctuations in the environment of the OH-stretching mode (i.e., acetonitrile molecules). The slow time scale coincides nicely with the rotational diffusion time that was determined in section 3. This proves that a water molecule that is hydrogen bonded to acetonitrile rotates independently of an acetonitrile molecule, and therefore, the hydrogen bond is broken within ∼2 ps.

Thus, for an originally non-water-bonded OH oscillator two ways of energy relaxation are possible. Relaxation occurs on a time scale of 12 ps when the corresponding OH group is

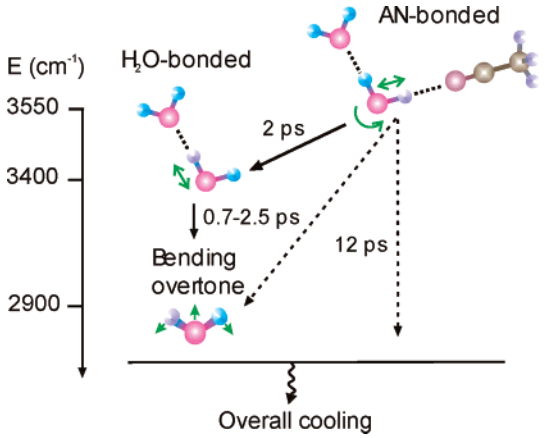

Figure 12. Schematic representation of the energy relaxation pathways for the OH-stretch vibrational mode of water molecules in acetonitrile solution.

completely isolated from any other water molecule. However, when the OH oscillator belongs to the water molecule that takes part in a cluster, the molecule can rotate within 2.5 ps to form a hydrogen bond to another water molecule with a subsequent relaxation at a subpicosecond time scale. Therefore, the total relaxation rate is equal to the sum of relaxation rates into both channels weighted with their respective concentrations

$$1/T_1^{\text{non-water-bonded}} = C^{\text{non-water-bonded}}/T_1^{\text{diluted}} + C^{\text{water-bonded}}/T_1^{\text{orientational}} \quad (6)$$

where $C^{\text{non-water-bonded}}$ and $C^{\text{water-bonded}}$ are concentrations of non-water-bonded and water-bonded hydroxyl groups, respectively, T_1^{diluted} is the population lifetime in diluted solution (∼12 ps), and $T_1^{\text{orientaitonal}}$ is the population lifetime in concentrated solution (∼ 2.5 ps). The results of simulations according to eq 6 describe the experimental data reasonably well (Figure 10).

The pathways of vibrational energy relaxation for the OH-stretching mode of HDO molecules in acetonitrile solution are schematically illustrated in Figure 12. Water-bonded OH oscillators relax through resonant energy transfer to the first overtone of the bending mode. With increasing water-cluster size the absorption spectrum broadens and shifts toward lower frequency. This ensures a greater overlap with the spectrum of the first overtone and subsequent lifetime shortening from ∼3 ps to ∼0.7 ps. For OH oscillators that have not been initially water bonded, there are two relaxation pathways. First, the oscillator can relax directly to the first overtone of a bending mode with a 12 ps lifetime. Second, the water molecule first rotates, then forms a hydrogen bond to a neighboring water molecule, becomes hydrogen bonded, and finally relaxes via resonance with the bending overtone. While the second path is much faster that the first one, it requires another water molecule in close proximity and therefore only becomes efficient at high concentrations.

Finally, we would like to compare our results on water−acetonitrile mixtures with similar experiments on methanol (ethanol) oligomers dissolved in carbon tetrachloride.[29−33,66] The main feature of the latter system is that vibrational relaxation of the excited OH (OD) stretching mode results in ultrafast breaking of the hydrogen bond at a time scale shorter than 2 ps. The broken hydrogen bond recovers at a time scale of ∼10 to 20 ps after which the temperature equilibration of the sample settles up. Our data on water−acetonitrile mixtures give no indication of intermediate hydrogen bond breaking and its subsequent recovery. Let us assume, for the sake of argument,

that the hydrogen bond is broken during or right after the vibrational relaxation. This would result in a signal decrease around 3400 cm^{-1} where the hydrogen-bonded molecules absorb and in a simultaneous induced absorption around 3550 cm^{-1}. However, there is no signature of such processes in the experimental data (Figure 7). Furthermore, the subsequent restoration of the broken hydrogen bond results in the opposite trends in the pump−probe signals,[29] again in clear contradiction with our experimental data. In contrast, the proposed model explains self-consistently the transient absorption data (Figures 5 and 7) and absorption spectra (Figure 8), and yields predictions on the mixture composition that are in accord with MD simulations (Figure 9).

We believe that the fundamental difference between relaxation dynamics in water−acetonitrile and methanol−carbon tetrachloride mixtures originates from the following two facts. First, H_2O as well as HDO are unique in the sense that there is an efficient energy relaxation channel into the bending mode.[2,3] Therefore, the energy is quickly redistributed among lower frequency modes with no hydrogen-bond dissociation. Second, acetonitrile is, after water, the fastest polar solvent, where diffusive processes are completed within 2 ps. This facilitates an energy flux from the excited HDO molecule to the solvent. In contrast, the buildup of bath excitation for carbon tetrachloride occurs at an ∼20 ps time scale.[2]

Clearly, additional studies are needed to confirm the importance of these facts for solvent-dependent vibrational dynamics. One obvious set of experiments on methanol oligomers dissolved in acetonitrile is already underway.

7. Summary and Conclusions

Analysis of the combined time- and frequency-resolved pump−probe signals from binary water−acetonitrile mixtures has provided direct information on two types of OH groups in the binary water−acetonitrile mixture: OH groups with a hydrogen bond to other water molecules and OH groups with no hydrogen bond or hydrogen bonded to acetonitrile. Such a distinction is possible because these two types of oscillators have distinctly different frequency-lifetime signatures. The spectral bands for the corresponding types of hydroxyl groups have been obtained by performing simultaneous numerical analysis of the linear and transient absorption spectra. The relative fractions of water-bonded and non-water-bonded hydroxyl groups were then derived from these data. The obtained fractions are in good agreement with the results of MD simulations.

Our findings are summarized in Figure 11 and corroborate the earlier suggested model for vibrational relaxation of the OH-stretching mode.[2,3,23,25] According to this model vibrational relaxation from the excited OH-stretching mode occurs through resonant energy transfer to the overtone of the bending mode with subsequent intra- and intermolecular redistribution to lower frequency vibrational modes. Hydrogen bonding speeds up the relaxation process by broadening and shifting the OH-stretch absorption spectrum to lower frequencies. These spectral changes lead to a substantial increase in overlap with the spectrum of the energy-accepting mode, leading to an increase of the relaxation rate.

In water−acetonitrile binary mixtures the size of the water clusters grows with increasing water concentrations. As a result, the spectral band corresponding to water-bonded hydroxyl groups shifts to lower frequencies and broadens. Consequently, the population lifetime for this type of hydroxyl group decreases from ∼3.0 ps in dilute solution to ∼0.7 ps in pure water.

For isolated water molecules surrounded by acetonitrile, the relaxation channel to the bending mode overtone becomes inefficient because of a negligible overlap between the donor and acceptor spectra. As a consequence, the population lifetime for such hydroxyl groups increases to ∼12 ps. For non-water-bonded hydroxyl groups, which are situated on the outer surface of the water clusters or, in general, in the proximity of other water molecules, the rate of vibrational energy relaxation is mainly determined by molecular reorientations. In this case the rotating water molecule forms a hydrogen bond to another water molecule, which leads to the modification of the spectrum and relaxation according to the mechanism outlined for water-bonded hydroxyl groups. The rate-limiting step in this process is molecular reorientation that occurs at a 2 ps time scale.

Acknowledgment. This paper is dedicated by Douwe Wiersma to Gerry Small, a long-time friend and inspiring colleague in the field of condensed phase spectroscopy for decades. We greatly acknowledge financial support from FOM (Fundamenteel Onderzoek der Materie).

References and Notes

(1) Kenkre, V. M.; Tokmakoff, A.; Fayer, M. D. *J. Chem. Phys.* **1994**, *101*, 10618.
(2) Dlott, D. D. *Chem. Phys.* **2001**, *266*, 149.
(3) Lawrence, C. P.; Skinner, J. L. *J. Chem. Phys.* **2002**, *117*, 5827.
(4) Luzar, A. *J. Chem. Phys.* **2000**, *113*, 10663.
(5) Yeremenko, S.; Pshenichnikov, M. S.; Wiersma, D. A. *Chem. Phys. Lett.* **2003**, *369*, 107.
(6) Lawrence, C. P.; Skinner, J. L. *Chem. Phys. Lett.* **2003**, *369*, 472.
(7) Stenger, J.; Madsen, D.; Hamm, P.; Nibbering, E. T. J.; Elsaesser, T. *Phys. Rev. Lett.* **2001**, *87*, 027401.
(8) Stenger, J.; Madsen, D.; Hamm, P.; Nibbering, E. T. J.; Elsaesser, T. *J. Phys. Chem. A* **2002**, *106*, 2341.
(9) Fecko, C. J.; Eaves, J. D.; Loparo, J. J.; Tokmakoff, A.; Geissler, P. L. *Science* **2003**, *301*, 1698.
(10) Pshenichnikov, M. S.; Yeremenko, S.; Wiersma, D. A. 2D Photon-Echo Spectroscopy of Hydrogen-Bond Dynamics in Liquid Water. In *Femtochemistry and Femtobiology: Ultrafast Events in Molecular Science*, Proceedings of the 6th International Conference on Femtochemistry, Maison de la Chimie, Paris, France, July 6−10, 2003; Martin, M. M., Hynes, J. T., Eds.; Elsevier, 2004; pp 165−168.
(11) Asbury, J. B.; Steinel, T.; Stromberg, C.; Corcelli, S. A.; Lawrence, C. P.; Skinner, J. L.; Fayer, M. D. *J. Phys. Chem. A* **2004**, *108*, 1107.
(12) Nienhuys, H.-K.; Woutersen, S.; van Santen, R. A.; Bakker, H. J. *J. Chem. Phys.* **1999**, *111*, 1494.
(13) Graener, H.; Seifert, G.; Laubereau, A. *Chem. Phys.* **1993**, *175*, 193.
(14) Graener, H.; Seifert, G. *J. Chem. Phys.* **1993**, *98*, 36.
(15) Egorov, S. A.; Skinner, J. L. *J. Chem. Phys.* **1996**, *105*, 7047.
(16) Bakker, H. J. *J. Chem. Phys.* **1993**, *98*, 8496.
(17) Moore, P.; Tokmakoff, A.; Keyes, T.; Fayer, M. D. *J. Chem. Phys.* **1995**, *103*, 3325.
(18) Nitzan, A.; Mukamel, S.; Jortner, J. *J. Chem. Phys.* **1974**, *60*, 3929.
(19) Tokmakoff, A.; Sauter, B.; Fayer, M. D. *J. Chem. Phys.* **1994**, *100*, 9035.
(20) Whitnell, R. M.; Wilson, K. R.; Hynes, J. T. *J. Chem. Phys.* **1992**, *96*, 5354.
(21) Velsko, S.; Oxtoby, D. W. *J. Chem. Phys.* **1980**, *72*, 2260.
(22) Tokmakoff, A.; Urdahl, R. S.; Zimdars, D.; Francis, R. S.; Kwok, A. S.; Fayer, M. D. *J. Chem. Phys.* **1995**, *102*, 3919.
(23) Deak, J. C.; Rhea, S. T.; Iwaki, L. K.; Dlott, D. D. *J. Phys. Chem. A* **2000**, *104*, 4866.
(24) Lock, A. J.; Bakker, H. J. *J. Chem. Phys.* **2002**, *117*, 1708.
(25) Rey, R.; Hynes, J. T. *J. Chem. Phys.* **1996**, *104*, 2356.
(26) Vodopyanov, K. L. *J. Chem. Phys.* **1991**, *94*, 5389.
(27) Graener, H.; Ye, T. Q.; Laubereau, A. *J. Chem. Phys.* **1989**, *91*, 1043.
(28) Staib, A.; Hynes, J. T. *Chem. Phys. Lett.* **1993**, *204*, 197.
(29) Gaffney, K. J.; Davis, P. H.; Piletic, I. R.; Levinger, N. E.; Fayer, M. D. *J. Phys. Chem. A* **2002**, *106*, 12012.
(30) Bonn, M.; Bakker, H. J.; Kleyn, A. W.; van Santen, R. A. *Phys. Chem.* **1996**, *100*, 15301.
(31) Laenen, R.; Gale, G. M.; Lascoux, N. *J. Phys. Chem. A* **1999**, *103*, 10708.

(32) Graener, H.; Ye, T. Q.; Laubereau, A. *J. Chem. Phys.* **1989**, *90*, 3413.
(33) Asbury, J. B.; Steinel, T.; Stromberg, C.; Gaffney, K. J.; Piletic, I. R.; Fayer, M. D. *J. Chem. Phys.* **2003**, *119*, 12981.
(34) Green, J. L.; Lacey, A. R.; Sceats, M. G. *J. Phys. Chem.* **1986**, *90*, 3958.
(35) Woutersen, S.; Bakker, H. J. *Nature* **1999**, *402*, 507.
(36) Lock, A. J.; Woutersen, S.; Bakker, H. J. *J. Phys. Chem. A* **2001**, *105*, 1238.
(37) Pakoulev, A.; Wang, Z.; Dlott, D. D. *Chem. Phys. Lett.* **2003**, *371*, 594.
(38) Pakoulev, A.; Wang, Z.; Pang, Y.; Dlott, D. D. *Chem. Phys. Lett.* **2003**, *380*, 404.
(39) Bakker, H. J.; Lock, A. J.; Madsen, D. *Chem. Phys. Lett.* **2004**, *385*, 329.
(40) Pakoulev, A.; Wang, Z.; Pang, Y.; Dlott, D. D. *Chem. Phys. Lett.* **2004**, *385*, 332.
(41) Lindner, J.; Vohringer, P.; Cringus, D.; Milder, M.; Pshenichnikov, M. S.; Wiersma, D. A. In preparation.
(42) Acosta, J.; Arce, A.; Rodil, E.; Soto, A. *Fluid Phase Equilib.* **2002**, *203*, 83.
(43) Bergman, D. L.; Laaksonen, A. *Phys. Rev. E* **1998**, *58*, 4706−4715.
(44) Bertie, J. E.; Lan, Z. *J. Phys. Chem. B* **1997**, *101*, 4111.
(45) Jamroz, D.; Stangret, J.; Lindgren, J. *J. Am. Chem. Soc.* **1993**, *115*, 6165.
(46) Kovacs, H.; Laaksonen, A. *J. Am. Chem. Soc.* **1991**, *113*, 5596.
(47) Moreau, C.; Douheret, G. *Thermochim. Acta* **1975**, *13*, 385.
(48) Mountain, R. D. *J. Phys. Chem. A* **1999**, *103*, 10744.
(49) Nigam, S.; Juan, A. d.; Stubbs, R. J. *Anal. Chem.* **2000**, *72*, 1956.
(50) Jellema, R.; Bulthuis, J.; van der Zwan, G. *J. Mol. Liq.* **1997**, *73*−*74*, 179.
(51) Satoh, Y.; Nakanishi, K. *Fluid Phase Equilib.* **1995**, *104*, 41.
(52) Shin, D. N.; Wijnen, J. W.; Engberts, J. B. F. N.; Wakisaka, A. *J. Phys. Chem. B* **2002**, *106*, 6014.
(53) Venables, D. S.; Schmuttenmaer, C. A. *J. Chem. Phys.* **1998**, *108*, 4935.
(54) Venables, D. S.; Schmuttenmaer, C. A. *J. Chem. Phys.* **2000**, *113*, 11222.
(55) Zhang, D.; Gutow, J. H.; Eisenthal, K. B.; Heinz, T. F. *J. Chem. Phys.* **1993**, *98*, 5099.
(56) Eaton, G.; Pena-Nunez, A. S.; Symons, M. C. R. *J. Chem. Soc., Faraday Trans.* **1988**, *84*, 2181.
(57) Herzberg, G. *Infrared and Raman Spectra of Polyatomic Molecule*; Krieger: New York, 1991.
(58) Hare, D. E.; Sorensen, C. M. *J. Chem. Phys.* **1990**, *93*, 6954.
(59) Gordon, R. G. *J. Chem. Phys.* **1966**, *45*, 1643.
(60) Bakker, H. J.; Woutersen, S.; Nienhuys, H.-K. *Chem. Phys.* **2000**, *258*, 233.
(61) von Jena, A.; Lessing, H. E. *Appl. Phys.* **1979**, *19*, 131.
(62) Marti, J.; Padro, J. A.; Guardia, E. *J. Chem. Phys.* **1996**, *105*, 639.
(63) Benson, S. W.; Siebert, E. D. *J. Am. Chem. Soc.* **1992**, *114*, 429.
(64) Franks, F. *Water: A Comprehensive Treatise*; Plenum Press: New York, 1972.
(65) de Boeij, W. P.; Pshenichnikov, M. S.; Wiersma, D. A. *J. Phys. Chem.* **1996**, *100*, 11806.
(66) Laenen, R.; Rauscher, C. *J. Chem. Phys.* **1997**, *106*, 8974.